[redacted]

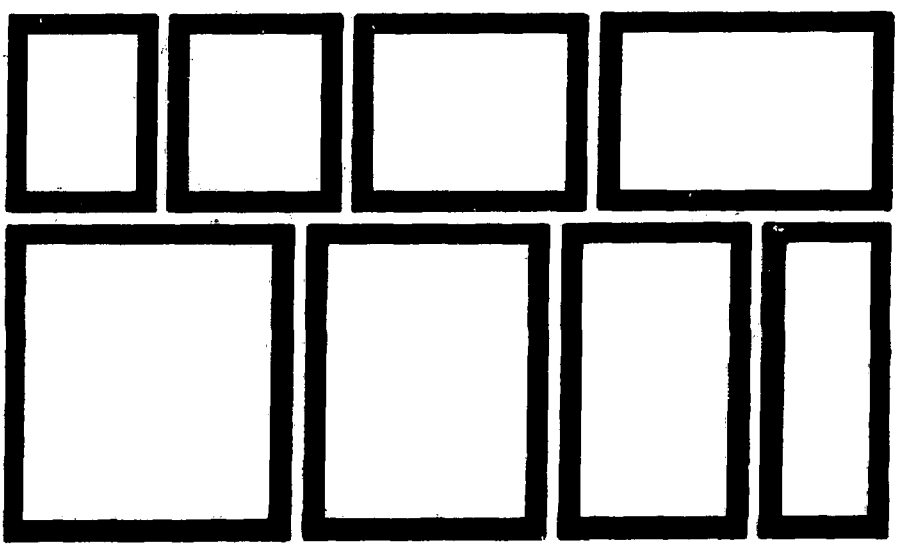

UNIT TENAGA NUKLEAR, JABATAN PERDANA MENTERI.

NUCLEAR ENERGY UNIT, PRIME MINISTER'S DEPARTMENT.

MALAYSIA

NEUTRON FLUX MEASUREMENTS IN PUSPATI TRIGA REACTOR

by

Gui Ah Auu
Mohd Amin Sharifuldin Salleh
Mohd Ali Sufi

Paper Presented at the
IAEA Seminar On Effective Utilization
and Management of Research Reactor
7-11 November, 1983
Kuala Lumpur
MALAYSIA

NEUTRON FLUX MEASUREMENTS IN PUSPATI TRIGA REACTOR

Gui Ah Auu, Mohd Amin Sharifuldin Salleh, Mohd Ali Sufi*

Reactor Department

*Research and Development

PUSPATI

MALAYSIA.

Abstract

Neutron flux measurement in the PUSPATI TRIGA Reactor (PTR) was initiated after its commissioning on 28 June 1982. Initial measured thermal neutron flux at the bottom of the rotary specimen rack (rotating) and in-core pneumatic terminus were 3.81E+11 n/cm^2 sec and 1.10E + 12 n/cm^2-sec respectively at 100KW. Work to complete the neutron flux data are still going on. The cadmium ratio, thermal and epithermal neutron flux are measured in the reactor core, rotary specimen rack, in-core pneumatic terminus and thermal column. Bare and Cadmium covered gold foils and wires are used for the above measurements. The activities of the irradiated gold foils and wires are determined using Ge(Li) and hyperpure germinium detectors.

Introduction

At present the PUSPATI TRIGA reactor are loaded with 83 standard fuel-moderator elements, 3 fuel follower control rods and 33 graphite dummy fuel element in the outermost ring (G-ring). The active section of standard fuel-moderator element is 15 in. long and 1.43 in. in diameter and contains approximately 8.5% uranium by weight enriched to 20% in U-235. The enriched uranium combined homogeneously with a zirconium hydride moderator. The core component, detectors, and fuel element arrangement are shown in figure 1.

The aim of the flux measurement project is to determine the neutron flux data at any possible position used by the experimenter for calculation or reference. The project is still under progress because of lack of personnel and time. Some results obtained from the previous measurement are reported here.

We also intend to measure the neutron flux with other foil or wire detectors to compare with the results obtained using the gold detectors after the measurement made by gold detectors are completed. At the moment we do not have any suitable detector for this purpose.

Instrumentation and Procedure

The neutron flux in the speciment rotary rack and the reactor core were measured with 4mm long 0.25mm diameter gold wires. In the thermal column 12.5mm diameter and 0.025mm thick gold foils were used instead. The mass of each wire and foil was about 3.5mg and 63mg respectively. The neutron flux measurement was made by irradiating the bare gold wire or foil and cadmium covered gold of the same geometry under the same operating conditions. All the materials were supplied by Reactor Experiments Inc. and claimed to be 99.995% pure.

The gold wires or foils were weighted by using very high accuracy Cahn electronic microbalance. The balance was calibrated by using a high precision 200mg weight with 5.4 microgram uncertainty. The irradiation time normally varies from 15 to 30 minutes depending on the irradiation location and power. The irradiation time of some Cadmium covered foils in the thermal column was increased to 2 hours in order to obtain sufficient foil activity. The irradiation time kept longer than 15 minutes to reduce the irradiation t error.

After the irradiation, the detectors, if found to be too active, were normally cooled for few days to eliminate the unneccessary dose from the cadmium cover and all the short halflive radio-activation product.

The activity of the gold wires were measured using Nuclear Data 6600 system. The ND6600 data aquisition system consists of 4096 channels Analogue to Digital converter, preamplifier, amplifier, terminal, deck writer and a hyperpure Germinium detector. The gold foil activities were measured using Ortec 7010 MCA system with Ge(Li) detector.

The standard source used for the system efficiency and energy calibration were bought from Amersham with uncertainties of about 3% to 5%. It is in the form of sealed point source manufactured on 1st June 1982.

The hyperpure Germinium resolution was less than 2.0 keV at half maximum for gold photopeak (412keV) which can be considered very good.

Analysis

The result shown here were calculated from irradiated gold wores and foils at stated reactor power and irradiation location in the PUSPATI TRIGA reactor by using the well known technique of bare and cadmium covered gold detectors. The complete set of data so far as yet, is not available. The cadmium ratio, thermal and epithermal neutron flux values to be presented are defined as follow:-

a) Thermal neutron flux: The flux calculated from specific activity of bare detector minus the specific activity of the cadmium covered detector. The flux values obtained were for neutrons with energies below

the cadmium cut-off energy (0.5eV).

b) Epithermal neutron flux: The flux calculated from the specific activity measured from the cadmium covered gold wire or foil detectors.

c) Cadmium Ratio: Calculated from the ratio of the specific activity of the bare detectors to the cadmium covered detectors.

Uncertainty

The error presented only include those due to system efficiency, counting statistic, and detector weight. In the flux calculation the correction for self shielding and flux depression were taken into account but the errors on correction factors were assumed to be small.

Result

The neutron flux measurements were made at the following positions:-

1. Eight axial location (top grid plate to bottom grid plate) for each ring at position B1, C2, D2, E2, F2 and G2.

2. Ten positions of the Rotary specimen rack (bottom part).

3. The seven removable stringers of the thermal column The results are presented in the from of graphs and tables.

a) Incore

Due to the difficulty of insertion of the gold detector into the flux holes on the grid plate which are 0.03 in. in diameter the flux measurements in the core were made by replacing the fuel element with a perspex rod which hold the wire detectors at the required positions.

The axial flux distribution for thermal and epithermal neutrons as presented on Figure 2 and 3 respectively, show the normal cosine shape flux distribution. The axial flux distribution for fuel position D2, and E2 were distorted significantly. This is the effect of flux perturbation caused by the shim fuel follower control rod in the D1 position. The peak flux at the core centre is higher by about 250% compared to the core top or bottom. The axial cadmium ratio varies from 7 to 11 for ring B(B1) and from 11 to 16 for the G(G2) ring.

The radial flux distribution for thermal and epithermal neutrons plotted on Figure 4 and Figure 5 respectively show the same cosine shap as the axial flux. The figure show similar distortion of the flux shape at D2 position. The reason for this effect is the same as above. B ring showed 300% higher in flux compared to the G ring. The position 24cm, 40cm, 46cm and 52cm shown on the graph were measured from the bottom grid plate. The radial cadmium ratio varies from 7 to 11, 11 to 16 and 7 to 10 for positions 52cm, 10cm and 34cm (in the middle of the core) from the bottom grid plate, respectively.

b) Rotary Specimen Rack (Lazy Susan)

The rotary specimen rack (often referred to as the Lazy Susan) assembly is located in an annular well in the reflector assembly immediately surrounding the top potion of the core. The rack supports 40 evenly spaced tubular aluminium containers that serve as receptacles for the specimen container. Each

position capable of accomodating two irradiation tubes that can be screwed together except for position 1. Ten positions were selected for measurement. Those positions were 1, 5, 9, 13, 17, 21, 25, 29, 33 and 37. The flux distribution in these positions were plotted in figure 6. As expected the ratio of thermal to epithermal flux is higher in the specimen rack compared to the ratio in the core. The variation of thermal and epithermal flux in these ratio varies from 8 to 10. This is due to the various different structure around the rotary specimen rack. These flux measurements were made at 100Kwatt reactor power level and the rack is not rotated. A 2.5 Curie neutron source was located between fuel locations F7, F6, G8 and G7 and very close to position number 37 of the rotary specimen rack.

c) Thermal Column

Figure 7 shown the thermal column irradiation facility at PUSPATI TRIGA reactor. Its dimensions are 122cm height, 122cm width and 127cm lenght. The facility has seven removal strings namely G7, L7, C7, J4, J10, E4 and E10. G7 is located in the middle and the other six are positioned symetrically around the central stringer.

Both thermal and epithermal flux measured were plotted in figure 8. Only the result for stringer G7, E10, C7 and L7 were plotted. The results for J10, J4 and E4 is quiet similar to E10. The cent centre stringer exhibit good agreement with exponetial flux variation as indicated by flux seemed to decrease at a faster rate than the thermal flux due to neutron thermalization as it travels away from the thermal column inner end. Since the number of neutrons captured is less than those being thermalized, there is a rapid rise in thermal to epithermal ratio as shown in figure 9. The cadmium ratio measured was in the range of 200 to 1000. Therefore the PTR thermal column can be considered as a very well thermalized neutron source.

Future Measurement and Program

In the future it is expected that a better gold detector such as very thin gold foil and dilute gold foils will be used, to eliminate the need for flux depression and self-shielding corrections. It is proposed that 4pi beta-gamma coincident counting system should be used for absolute flux measurement. Different types of foil detectors will be used to compare the results obtained.

Neutron temperature measurement will be carried out when lutetium foils are available. Neutron spectrum measurement at various experimental facilities using threshold foils will be initiated in the near future.

References:

1. I.A.E.A Technical Reports Series No.107.
   Neutron Fluence Measurements.

2. Nuclear Data Guide for Reactor Neutron Metrology
   Commission of the European Communities

3. TRIGA Mk II Mechanical Operation and Maintenance Manual.

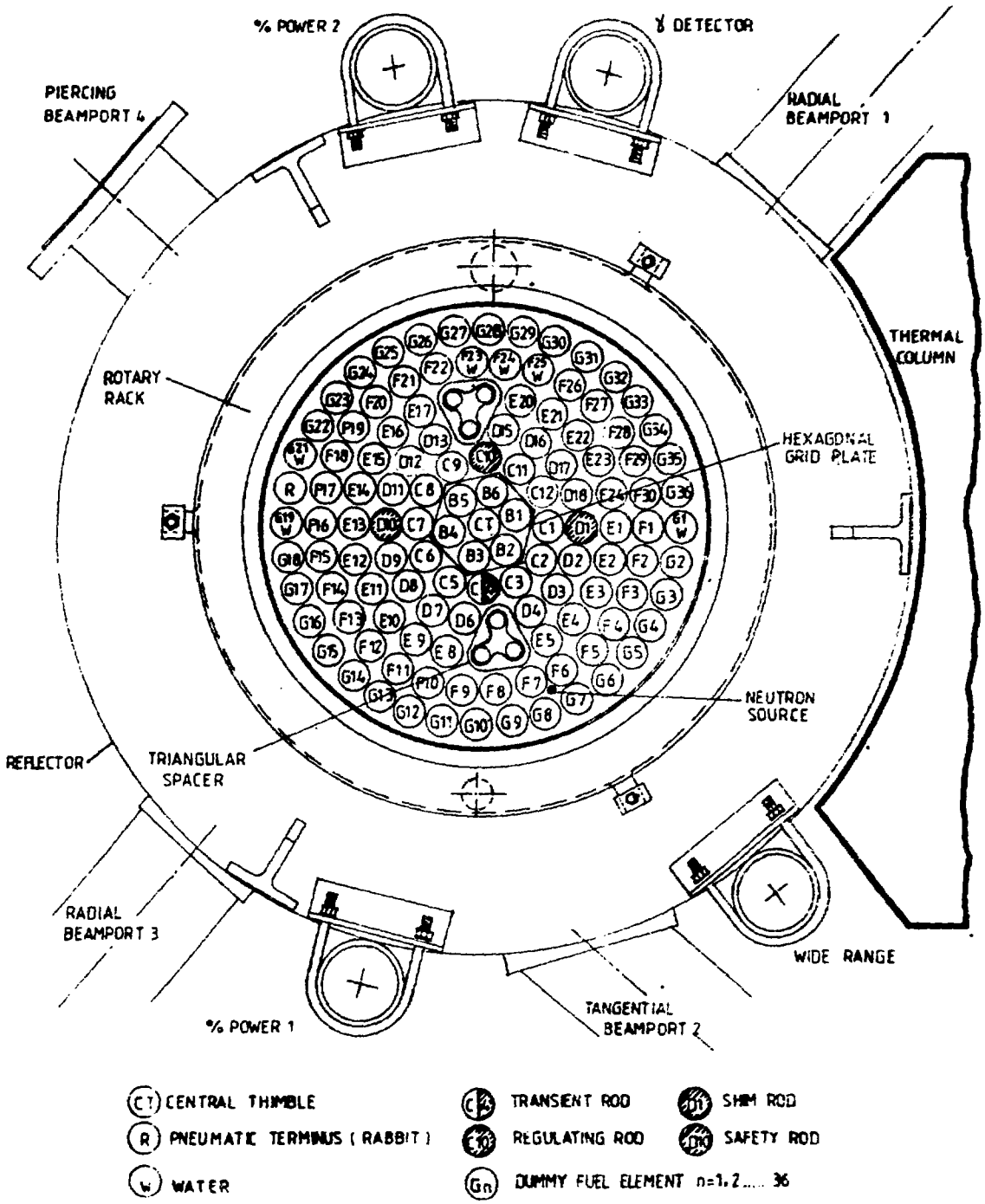

Figure 1 . Plan view of PTR experimental facilities .

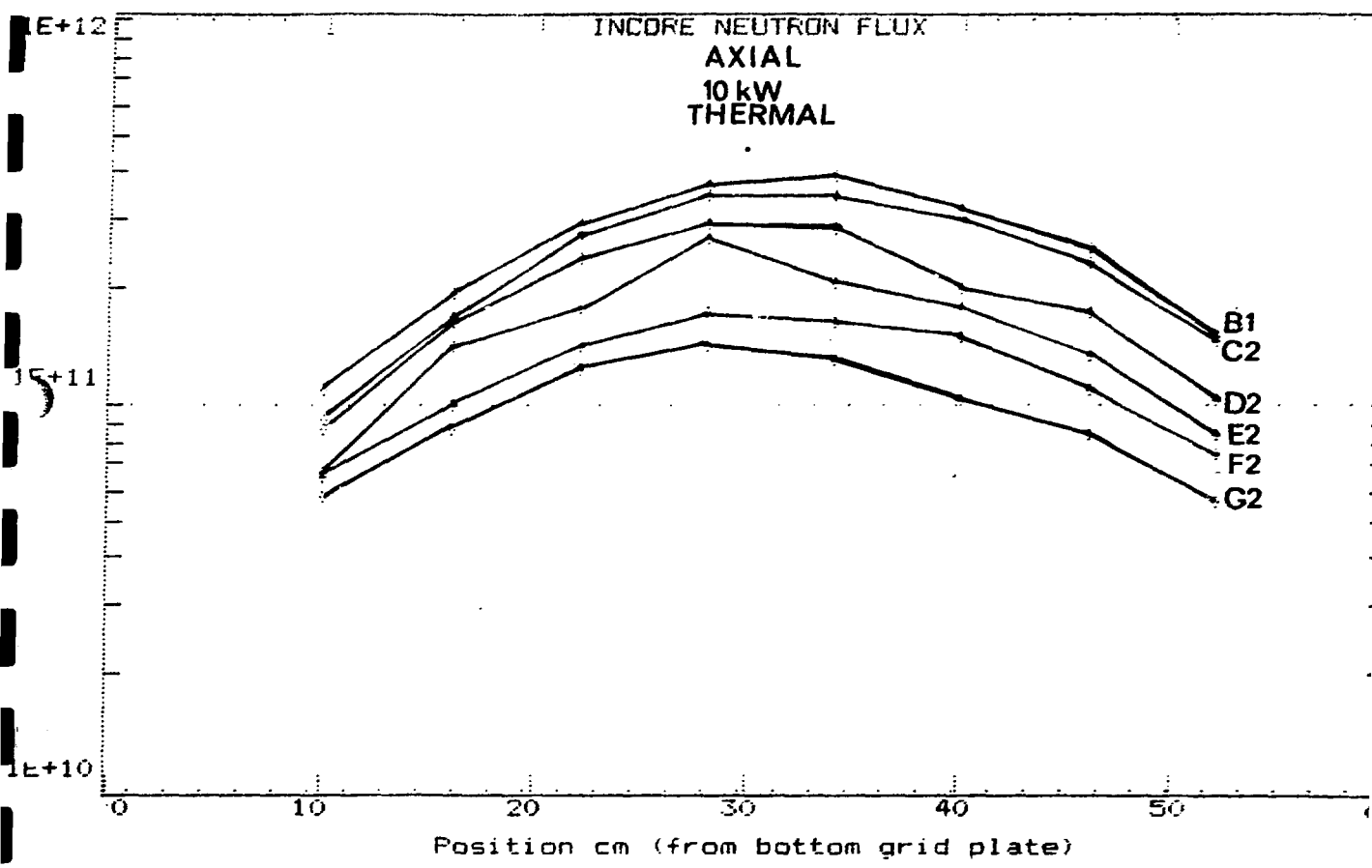

Figure:2 Axial Incore Thermal Flux

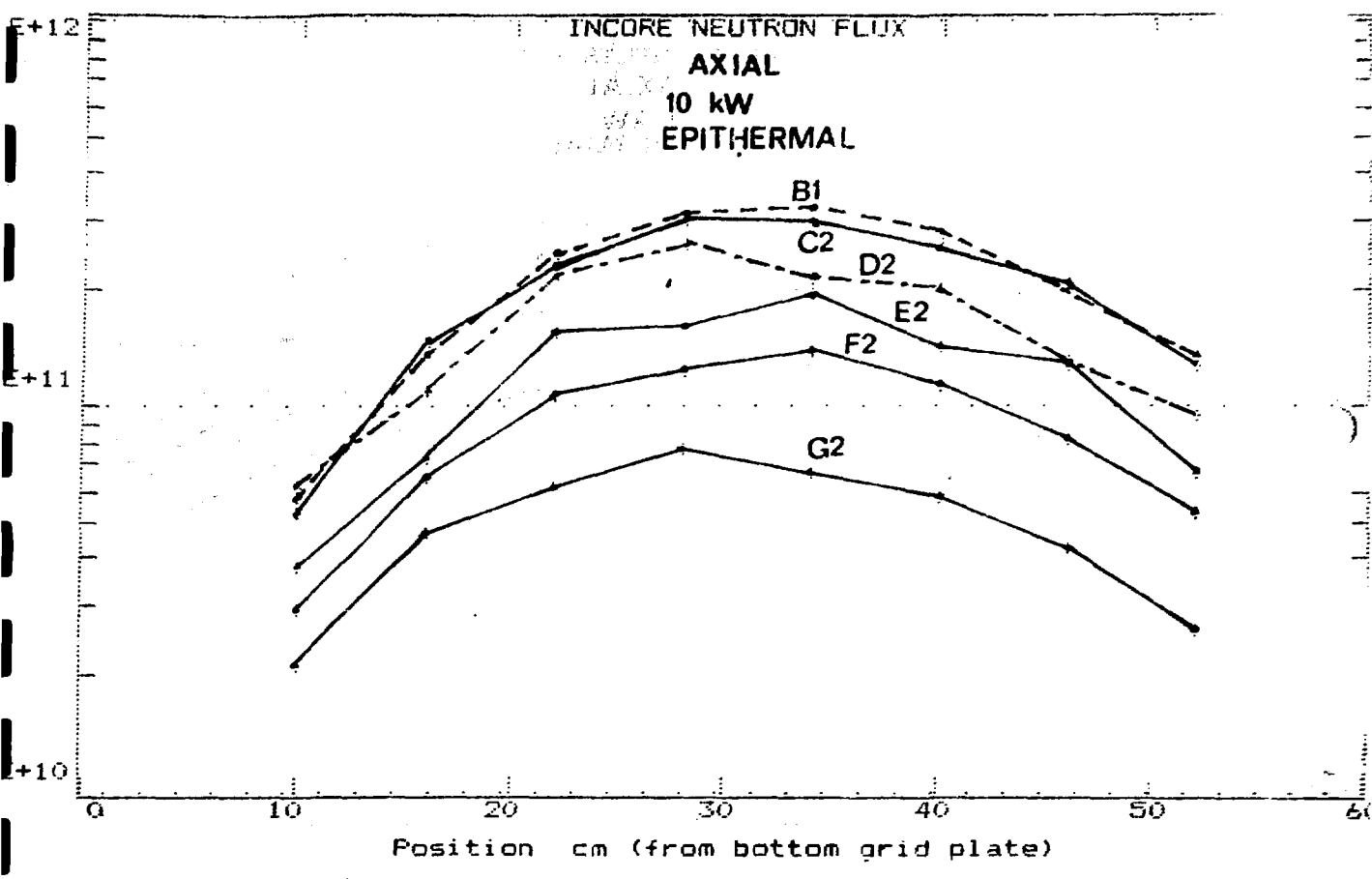

Figure: 3 Axial Incore Epithermal Flux

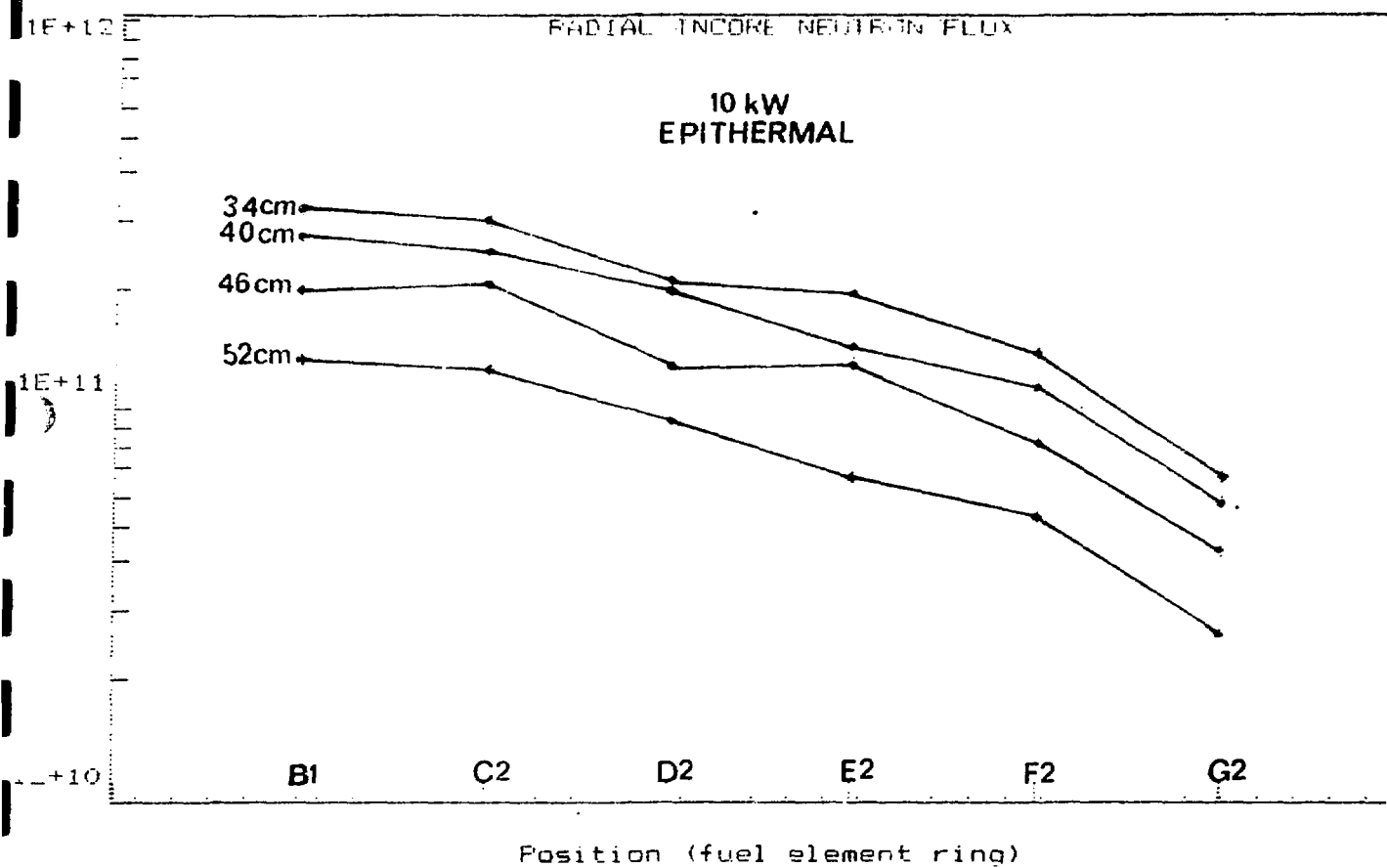

Figure : 4 Radial Incore Epithermal Flux

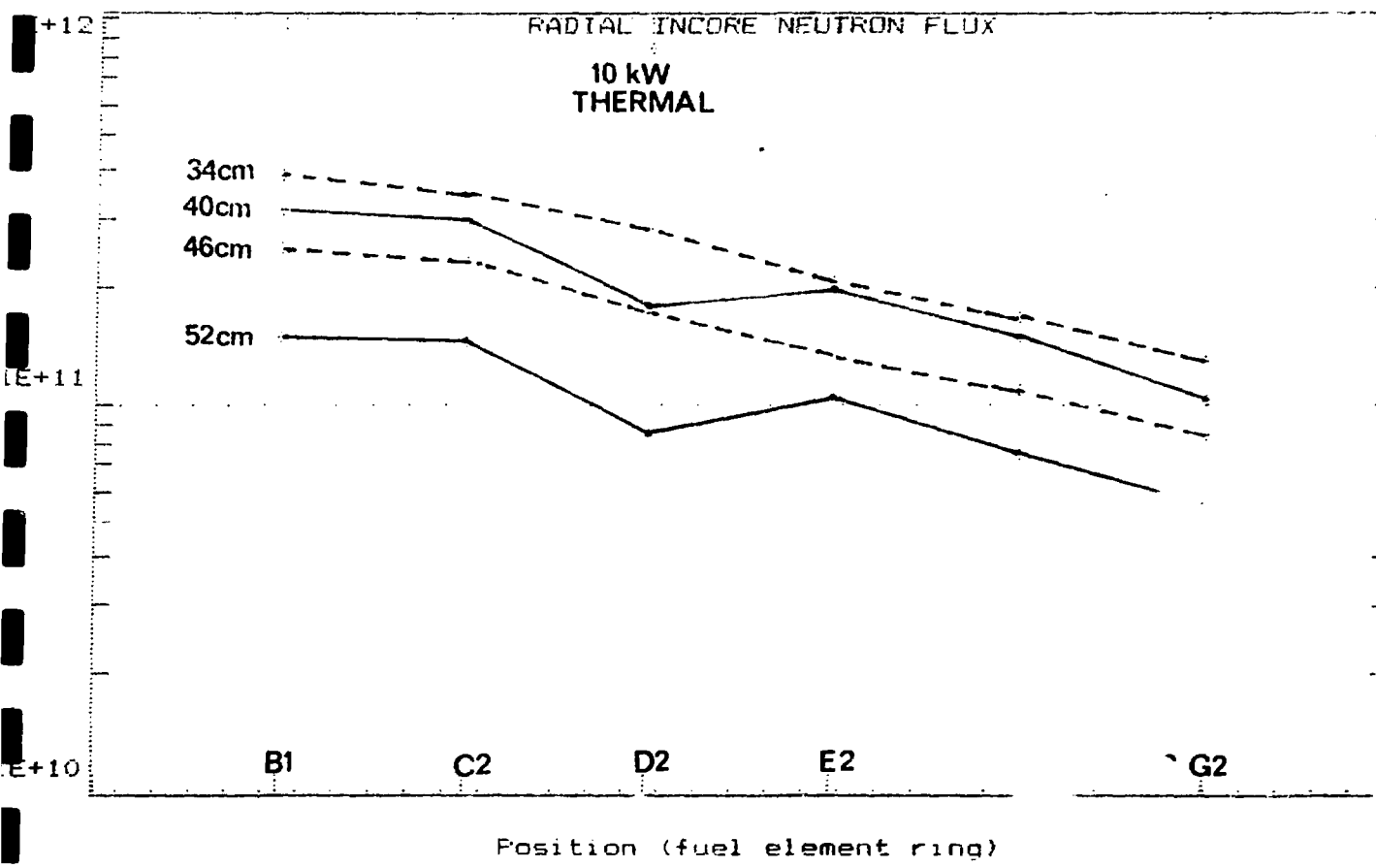

Figure :5 Radial Incore Thermal Flux

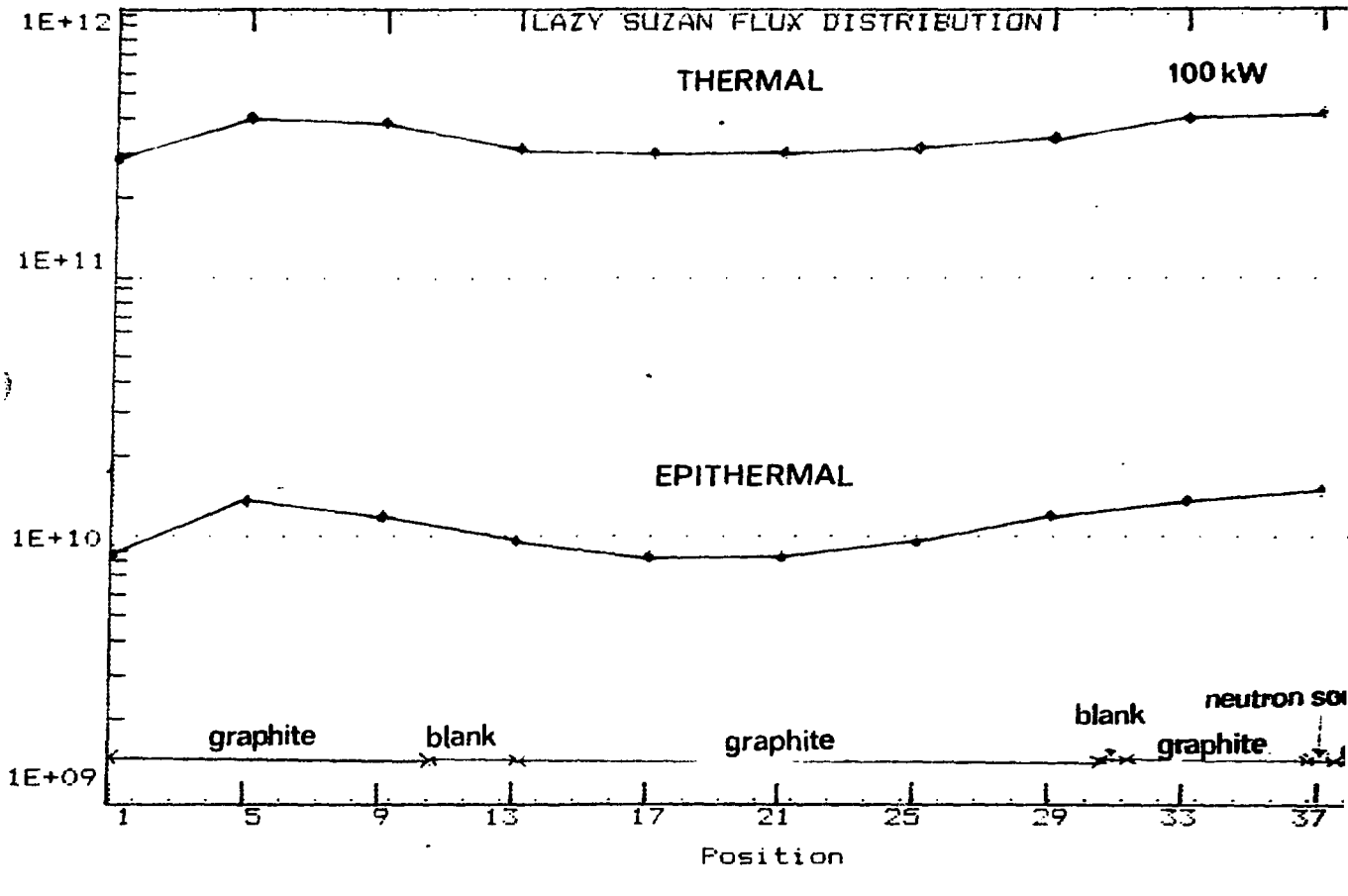

Figure:6 Lazy Susan Flux Distribution

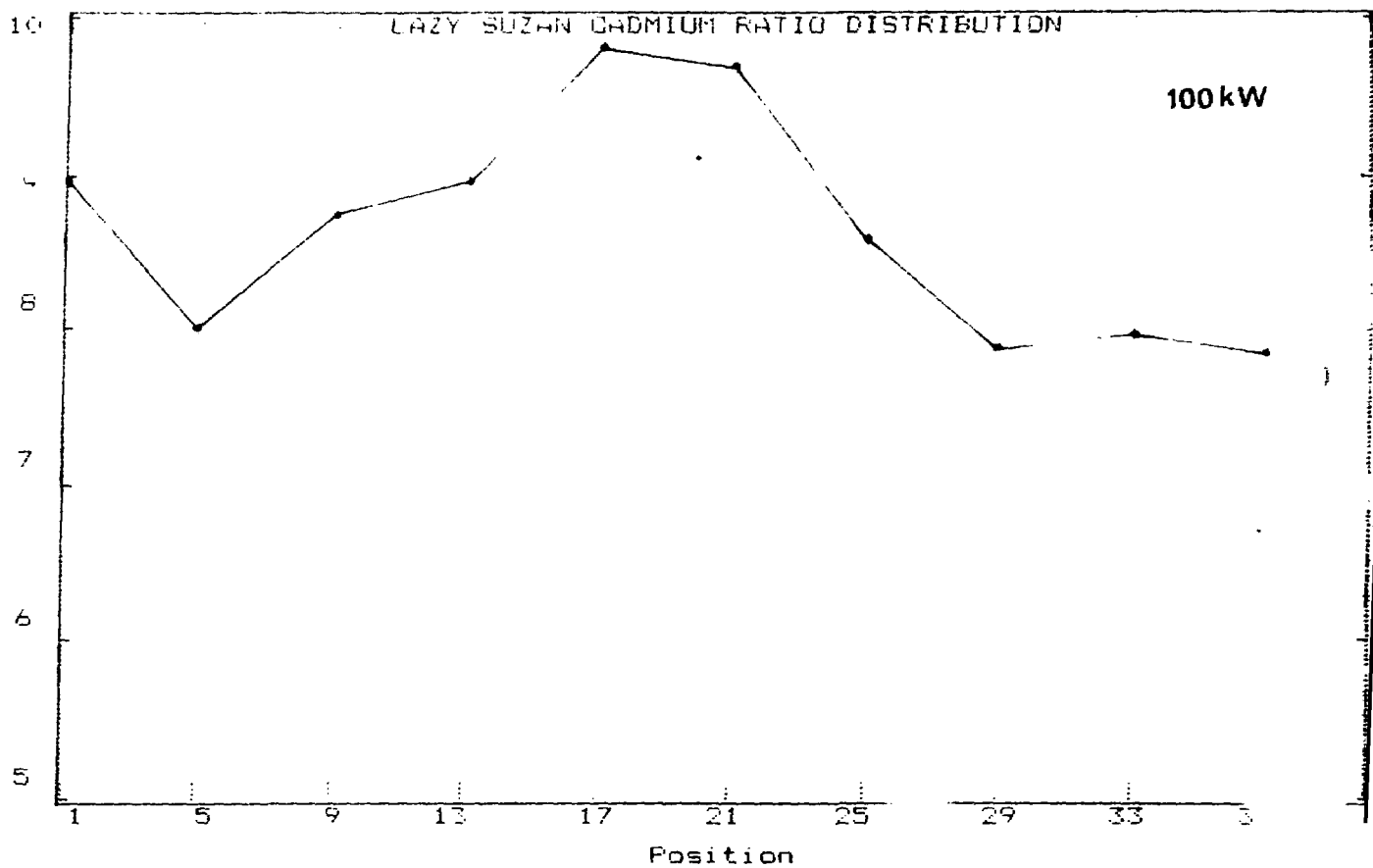

Figure:7 Lazy Susan Cadmium ratio Distribution

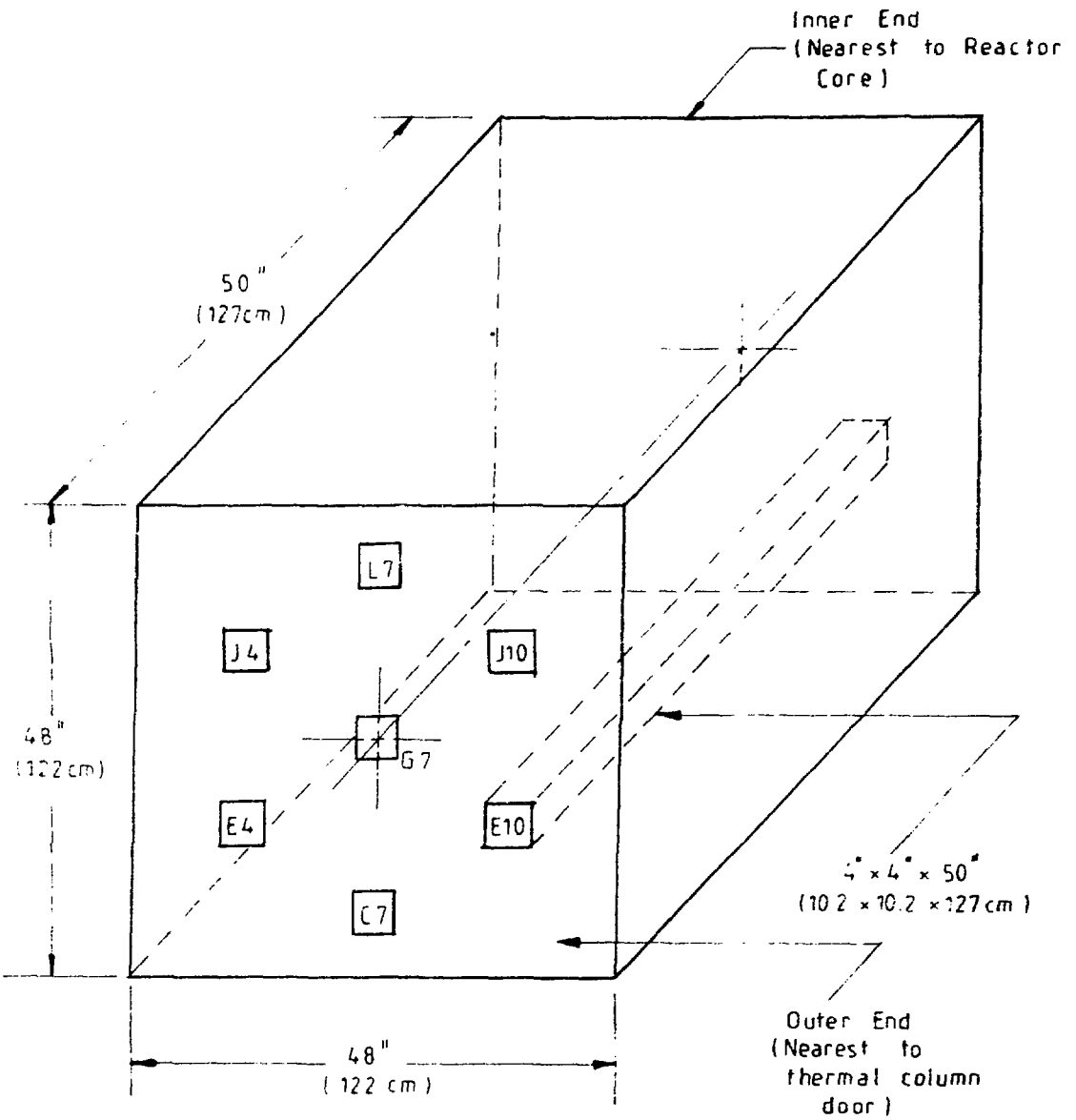

Fig. 8 Removal stringers in the thermal column.

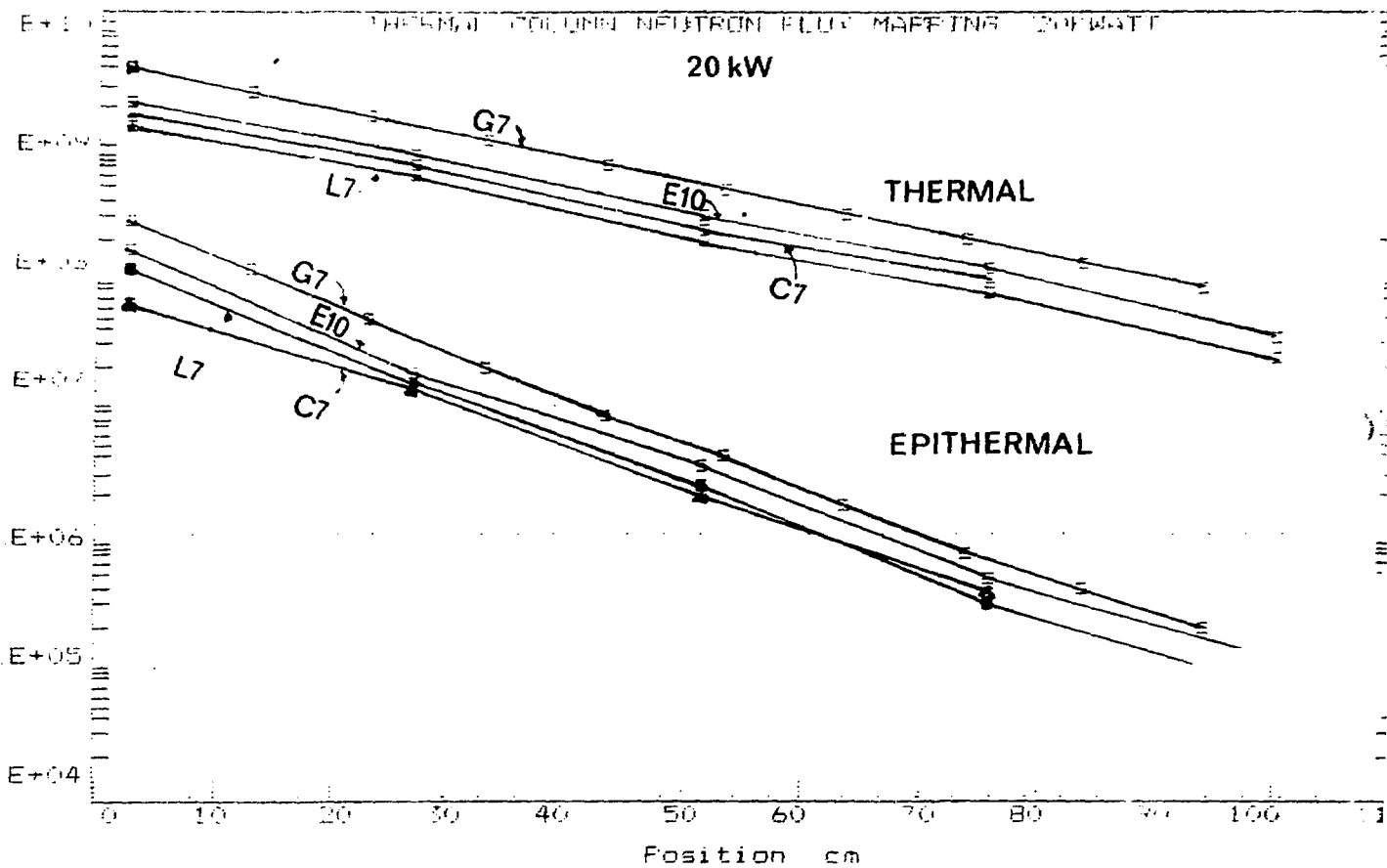

Figure: 9 Thermal Column Neutron Flux Mapping

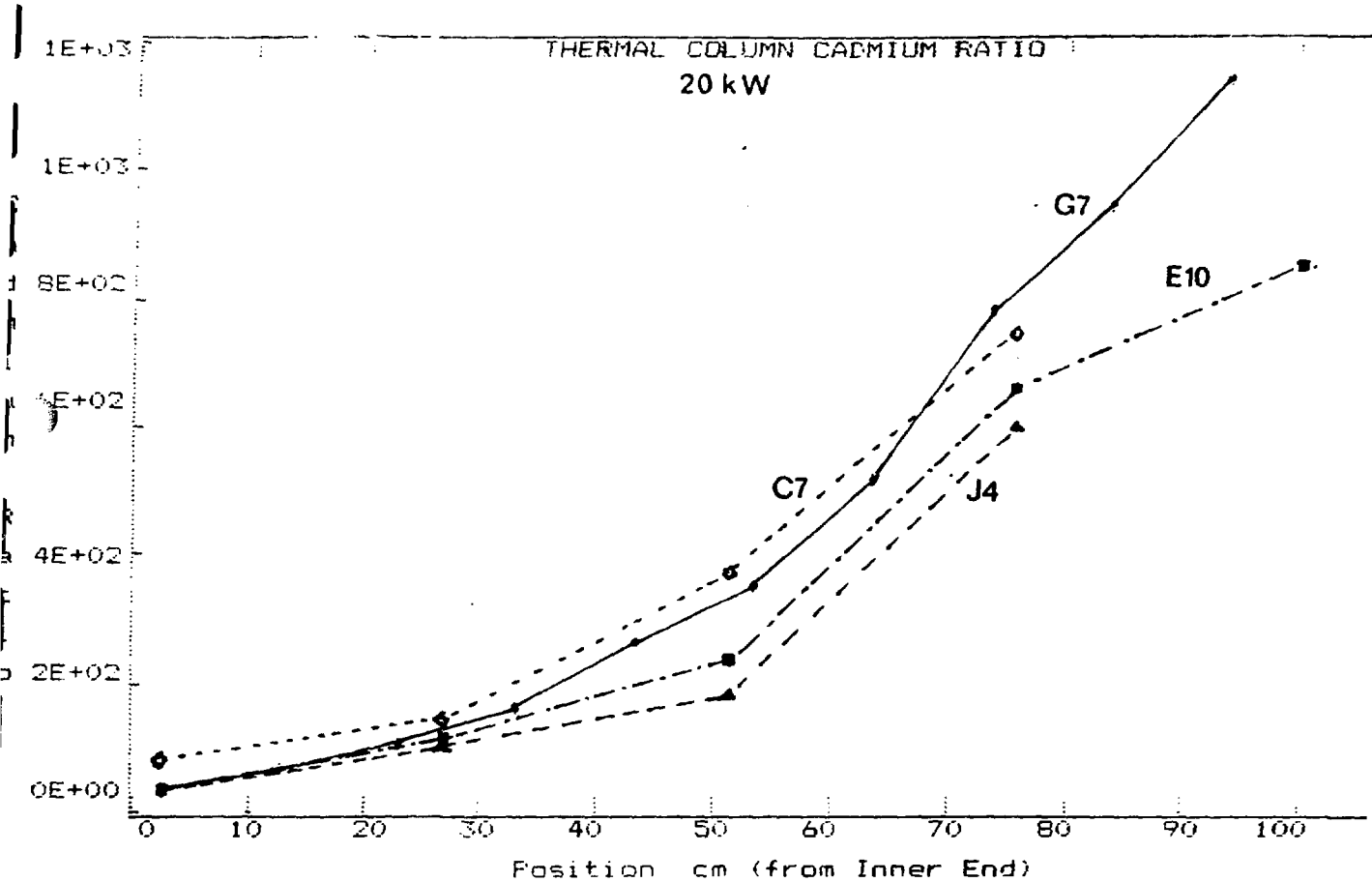

Figure: 10 Thermal Column Cadmium Ratio

KTR Incore Flux

Reactor Power = 10kW

Table: 1

Position	Position (from bottom grid plate) (cm)	Cadmium Ration	Øth ($n/cm^2/sec$)	Øepi (n/cm^2 - sec)
B1	52	7.1 ± 0.5	(1.51 ± 0.09) x 10^{11}	(1.33 ± 0.14) x 10
	46	7.9 ± 0.5	(1.56 ± 0.14) x 10^{11}	(1.61 ± 0.1
	40	7.1 ± 0.5	(3.17 ± 0.18) x 10^{11}	(2.79 ± 0.28) x 10
	34	7.6 ± 0.5	(3.92 ± 0.21) x 10^{11}	(3.18 ± 0.32) x 10^{1}
	28	7.3 ± 0.5	(3.67 ± 0.21) x 10^{11}	(3.15 ± 0.32) x 10^{1}
	22	7.5 ± 0.5	(2.98 ± 0.17) x 10^{11}	(2.49 ± 0.25) x 1
	16	8.6 ± 0.6	(1.97 ± 0.11) x 10^{11}	(1.39 ± 0.14) x 10
	10	11.1 ± 0.8	(1.10 ± 0.06) x 10^{11}	(5.81 ± 0.57) x 10 ^{10}
C2	52	7.3 ± 0.5	(1.47 ± 0.08) x 10^{11}	(1.25 ± 0.13) x
	46	7.9 ± 0.5	(2.34 ± 0.14) x 10^{11}	(2.09 ± 0.
	40	7.3 ± 0.5	(3.01 ± 0.17) x 10^{1}	(2.56 ± 0.26) x 1
	34	7.1 ± 0.5	(3.47 ± 0.20) x 10^{1}	(3.05 ± 0.32) x 10^{11}
	28	7.2 ± 0.5	(3.48 ± 0.20) x 10^{11}	(3.00 ± 0.31) x 10^{11}
	22	7.5 ± 0.5	(2.75 ± 0.16) x 10^{11}	(2.33 ± 0.24) x 10^{11}
	16	7.4 ± 0.5	(1.70 ± 0.10) x 10^{11}	(1.45 ± 0.15) x 10^{11}
	10	10.4 ± 0.7	(9.24 ± 0.51) x 10^{10}	(5.29 ± 0.05) x 10^{10}
D2	52	5.8 ± 0.4	(8.41 ± 0.52) x 10^{10}	(9.43 ± 1.03) x 10^{10}
	46	8.3 ± 0.6	(1.73 ± 0.10) x 10^{11}	(1.28 ± 0.13) x 10^{11}
	40	5.8 ± 0.4	(1.79 ± 0.11) x 10^{11}	(1.99 ± 0.21) x 10^{11}

Position	Position (from bottom grid plate) (cm)	Cadmium Ratio	Øth (n/cm^2/sec)	Øepi (n/cm^2 - sec)
D2	34	6.1 ± 0.6	(2.13 ± 0.15) x 10^{11}	(2.14 ± 0.22) x 10^{11}
	28	7.1 ± 0.5	(2.94 ± 0.17) x 10^{11}	(2.56 ± 0.27) x 10^{11}
	22	6.8 ± 0.5	(2.37 ± 0.14) x 10^{11}	(2.19 ± 0.23) x 10^{11}
	16	9.1 ± 0.6	(1.65 ± 0.09) x 10^{11}	(1.10 ± 0.11) x 10^{11}
	10	7.6 ± 0.6	(8.61 ± 0.49) x 10^{10}	(6.08 ± 0.62) x 10^{10}
E2	52	4.4 ± 0.6	(1.02 ± 0.06) x 10^{11}	(6.68 ± 0.40) x 10^{10}
	46	6.1 ± 0.4	(1.34 ± 0.08) x 10^{11}	(1.29 ± 0.14) x 10^{11}
	40	7.8 ± 0.5	(1.99 ± 0.11) x 10^{11}	(1.42 ± 0.14) x 10^{11}
	34	6.0 ± 0.4	(2.06 ± 0.12) x 10^{11}	(1.98 ± 0.21) x 10^{11}
	28	9.0 ± 0.6	(2.67 ± 0.15) x 10^{11}	(1.61 ± 0.16) x 10^{11}
	22	6.6 ± 0.5	(1.79 ± 0.11) x 10^{11}	(1.56 ± 0.16) x 10^{11}
	16	10.4 ± 0.7	(1.40 ± 0.08) x 10^{11}	(7.23 ± 0.71) x 10^{10}
	10	9.1 ± 0.6	(6.45 ± 0.36) x 10^{10}	(3.86 ± 0.39) x 10^{10}
F2	52	8.7 ± 0.6	(7.49 ± 0.43) x 10^{10}	(5.26 ± 0.53) x 10^{10}
	46	8.1 ± 0.6	(1.08 ± 0.06) x 10^{11}	(8.18 ± 0.83) x 10^{10}
	40	8.3 ± 0.6	(1.51 ± 0.09) x 10^{11}	(1.11 ± 0.11) x 10^{11}
	34	7.3 ± 0.5	(1.63 ± 0.09) x 10^{11}	(1.38 ± 0.14) x 10^{11}
	28	8.6 ± 0.6	(1.74 ± 0.10) x 10^{11}	(1.23 ± 0.12) x 10^{11}
	22	8.1 ± 0.6	(1.40 ± 0.08) x 10^{11}	(1.07 ± 0.11) x 10^{11}
	16	9.16 ± 0.6	(9.86 ± 0.55) x 10^{10}	(6.50 ± 0.66) x 10^{10}
	10	11.4 ± 0.8	(5.77 ± 0.32) x 10^{10}	(2.98 ± 0.29) x 10^{10}

Position	Position (from bottom grid plate) (cm)	Cadmium Ration	ϕth ($n/cm^2/sec$)	ϕepi (n/cm^2 - sec)
G2	52	11.2 ± 0.8	(5.58 ± 0.31) x 10^{10}	(2.65 ± 0.26) x 10^{10}
	46	10.5 ± 0.7	(8.43 ± 0.47) x 10^{10}	(4.30 ± 0.43) x 10^{10}
	40	9.6 ± 0.6	(1.03 ± 0.06) x 10^{11}	(5.23 ± [illegible]
	34	10.6 ± 0.7	(1.31 ± 0.07) x 10^{11}	(6.60 ± 0.65) x [illegible]
	28	9.8 ± 0.7	(1.40 ± 0.08) x 10^{11}	(7.69 ± 0.76) x [illegible]
	22	10.9 ± 0.8	(1.22 ± 0.07) x 10^{11}	(6.07 ± 0.69) x 10^{10}
	16	10.0 ± 0.7	(9.65 ± 0.48) x 10^{10}	(4.66 ± 0.46) x [illegible]
	10	16.1 ± 1.0	(6.65 ± 0.35) x 10^{10}	(2.13 ± 0.20) x 10^{10}

AXIAL NEUTRON FLUX DISTRIBUTION

REACTOR POWER - 100 kW

Table: 2

Position	ϕ_{th} ($n/cm^2/sec$) Thermal	ϕ_{epi} ($n/cm^2/sec$) Epithermal	Cadmium Ration
1	[illegible]	[illegible]	[illegible]
5	[illegible]	[illegible]	[illegible]
9	$(3.79 \pm 0.22) \times 10^{11}$	[illegible]	[illegible]
13	$(3.09 \pm 0.18) \times 10^{11}$	$(9.53 \pm 0.60) \times 10^{9}$	[illegible]
17	$(3.00 \pm 0.17) \times 10^{11}$	$(8.40 \pm 0.53) \times 10^{9}$	9.8 ± 0.8
21	$(2.95 \pm 0.17) \times 10^{11}$	$(8.38 \pm 0.52) \times 10^{9}$	9.7 ± 0.8
25	$(3.04 \pm 0.17) \times 10^{11}$	[illegible]	[illegible]
29	$(3.86 \pm 0.19) \times 10^{11}$	[illegible]	7.9 ± 0.8
33	$(3.91 \pm 0.22) \times 10^{11}$	$(1.38 \pm 0.09) \times 10^{10}$	8.0 ± 0.8
37	$(4.22 \pm 0.24) \times 10^{11}$	$(1.51 \pm 0.10) \times 10^{10}$	7.9 ± 0.8

Thermal Column Neutron Flux

Reactor Power = 20 KW

Table: 3

Graphite Stringers Number	Position (cm)	Cadmium Ratio	Øth ($n/cm^2/sec$)	Øepi (n/cm^2 - sec)
G7	2.54	41.3 ± 3.3	$(4.10 \pm 0.23) \times 10^9$	$(2.83 \pm 0.24) \times 10^8$
	11.7	85.4 ± 3.6	$(2.71 \pm 0.15) \times 10^9$	$(1.20 \pm 0.10) \times 10^8$
	22.9	103 ± 6	$(1.75 \pm 0.10) \times 10^9$	$(4.91 \pm 0.41) \times 10^7$
	33.0	161 ± 9	$(1.14 \pm 0.06) \times 10^9$	$(2.03 \pm 0.17) \times 10^7$
	43.2	283 ± 1.6	$(7.51 \pm 0.42) \times 10^8$	$(8.17 \pm 0.70) \times 10^6$
	53.3	349 ± 22	$(4.89 \pm 0.28) \times 10^8$	$(4.00 \pm 0.36) \times 10^6$
	63.5	516 ± 34	$(3.07 \pm 0.18) \times 10^8$	$(1.70 \pm 0.16) \times 10^6$
	73.7	779 ± 51	$(2.02 \pm 0.12) \times 10^8$	$(7.08 \pm 0.67) \times 10^5$
	83.8	943 ± 95	$(1.25 \pm 0.07) \times 10^8$	$(3.78 \pm 0.45) \times 10^5$
	94.0	1137 ± 82	$(8.09 \pm 0.47) \times 10^7$	$(2.03 \pm 0.20) \times$
J4	2.54	31.6 ± 1.8	$(2.12 \pm 0.15) \times 10^9$	$(1.98 \pm 0.11) \times 10^6$
	26.9	109 ± 8	$(8.95 \pm 0.49) \times 10^8$	$(2.36 \pm 0.23) \times 10^7$
	51.3	179 ± 17	$(2.87 \pm 0.19) \times 10^8$	$(4.59 \pm 0.55) \times 10^6$
	75.5	598 ± 44	$(1.08 \pm 0.06) \times 10^8$	$(5.17 \pm 0.50) \times 10^5$
	100.1	1510 ± 151	$(3.32 \pm 0.23) \times 10^7$	$(6.26 \pm 0.65) \times 10^4$
E10	2.54	41.3 ± 3.6	$(2.28 \pm 0.16) \times 10^9$	$(1.61 \pm 0.19) \times 10^8$
	26.9	136 ± 8	$(8.93 \pm 0.49) \times 10^8$	$(1.88 \pm 0.16) \times 10^7$
	51.3	242 ± 58	$(3.05 \pm 0.21) \times 10^8$	$(3.61 \pm -.91) \times 10^6$
	75.7	662 ± 19	$(1.13 \pm 0.33) \times 10^8$	$(4.88 \pm 0.20) \times 10^5$
	100.1	850 ± 75	$(3.39 \pm 0.23) \times 10^7$	$(1.14 \pm 0.13) \times 10^5$

Graphite Stringers Number	Position (cm)	Cadmium Ration	Øth ($n/cm^2/sec$)	Øepi (n/cm^2 - sec)
E4	2.54	53.7 ± 3.0	(2.47 ± 0.14) x 10^9	(1.34 ± 0.11) x 10^8
	26.9	126 ± 12	(8.24 ± 0.56) x 10^8	(1.88 ± 0.22) x 10^7
	51.3	344 ± 22	(3.20 ± 0.18) x 10^8	(2.65 ± 0.23) x 10^6
	75.7	954 ± 77	(1.10 ± 0.07) x 10^8	(3.30 ± 0.36) x 10^5
	100.0	1065 ± 87	(3.49 ± 0.20) x 10^7	(9.35 ± 0.10) x 10^4
J10	2.54	41.6 ± 2.5	(2.31 ± 0.14) x 10^9	(1.62 ± 0.14) x 10^8
	26.9	95.6 ± 8.8	(7.79 ± 0.52) x 10^8	(2.34 ± 0.28) x 10^7
	51.3	320 ± 20	(2.97 ± 0.18) x 10^8	(2.65 ± 0.24) x 10^6
	75.7	756 ± 73	(1.00 ± 0.07) x 10^8	(3.79 ± 0.46) x 10^5
	100.1	847 ± 69	(3.46 ± 0.22) x 10^7	(1.17 ± 0.12) x 10^5
L7	2.54	37.0 ± 3.3	(1.44 ± 0.10) x 10^9	(1.14 ± 0.14) x 10^8
	26.9	114 ± 6	(5.91 ± 0.33) x 10^8	(1.49 ± 0.12) x 10^7
	51.3	236 ± 30	(1.98 ± 0.13) x 10^8	(2.40 ± 0.36) x 10^6
	75.7	699 ± 48	(7.61 ± 0.42) x 10^7	(3.11 ± 0.28) x 10^5
	100.1	1026 ± 110	(1.38 ± 0.16) x 10^7	(6.60 ± 0.86) x 10^4
C7	2.54	84.6 ± 4.7	(1.89 ± 0.11) x 10^9	(6.46 ± 0.54) x 10^7
	26.9	144 ± 14	(7.00 ± 0.47) x 10^8	(1.39 ± 0.17) x 10^7
	51.3	371 ± 22	(1.29 ± 0.15) x 10^8	(2.15 ± 0.18) x 10^6
	75.7	742 ± 57	(9.59 ± 0.65) x 10^7	(3.69 ± 0.39) x 10^5